ELSEVIER

Coordination Chemistry Reviews
190–192 (1999) 933–960

COORDINATION CHEMISTRY REVIEWS

www.elsevier.com/locate/ccr

Pt-catalyzed hydrosilylation of ethylene. A theoretical study of the reaction mechanism

Shigeyoshi Sakaki [a,*], Nobuteru Mizoe [a], Manabu Sugimoto [a], Yasuo Musashi [b]

[a] *Department of Applied Chemistry and Biochemistry, Faculty of Engineering, Kumamoto University, Kumamoto 860-8555, Japan*

[b] *Information Processing Center, Kumamoto University, Kumamoto 860-8555, Japan*

Received 4 September 1998; received in revised form 1 February 1999; accepted 6 April 1999

Contents

* Corresponding author. Tel.: +81-96-342-3651; fax: +81-96-342-3679.
E-mail address: sakaki@gpo.kumamoto-u.ac.jp (S. Sakaki)

0010-8545/99/$ - see front matter
PII: S0010-8545(99)00130-7

Abstract

All the elementary steps involved in platinum(0)-catalyzed hydrosilylation of ethylene were theoretically investigated in detail with ab initio MO/MP2-MP4(SDQ) and CCD methods. Several important results are summarized as follows: (1) the Si–H oxidative addition of silane to $Pt(PH_3)_2$ occurs with a very low barrier. (2) Ethylene is more easily inserted into Pt–H than into $Pt–SiR_3$ (R = H, Cl, or Me). (3) The Si–C reductive elimination from $Pt(CH_3)(SiR_3)(PH_3)(C_2H_4)$ and the C–H reductive elimination from $PtH(CH_3)(PH_3)(C_2H_4)$ occur more easily than those from $Pt(CH_3)(SiR_3)(PH_3)_2$ and $PtH(CH_3)(PH_3)_2$, respectively. (4) The transition state of the Si–C reductive elimination is non-planar, while that of the C–H reductive elimination is planar. From those results, the reaction mechanism of $Pt(PH_3)_2$-catalyzed hydrosilylation of ethylene was discussed. The rate-determining step of the Chalk–Harrod mechanism is the isomerization of ethylene insertion product whose barrier is estimated to be about 22 kcal mol^{-1} for R = H and Me, and 26 kcal mol^{-1} for R = Cl (MP4SDQ values are given here), while that of the modified Chalk–Harrod mechanism is the ethylene insertion into $Pt–SiR_3$ whose barrier is 44 kcal mol^{-1} for R = H, 41 kcal mol^{-1} for R = Me, and 60 kcal mol^{-1} for R = Cl. Thus, the Chalk–Harrod mechanism is more favorable than the modified Chalk–Harrod mechanism in the $Pt(PH_3)_2$-catalyzed hydrosilylation of ethylene. Though *cis*-$PtH(SiH_3)(PH_3)_2$ is directly produced by the SiH_4 oxidative addition to $Pt(PH_3)_2$, the *cis*-complex might isomerize to the *trans*-form through Berry's pseudo-rotation mechanism. Ethylene is much more easily inserted into Pt–H and $Pt–SiH_3$ in *trans*-$PtH(SiH_3)(PH_3)(C_2H_4)$ than in the *cis*-form. Even in the *trans*-form, ethylene is more easily inserted into Pt–H than into $Pt–SiH_3$. In the Chalk–Harrod and modified Chalk–Harrod mechanisms including the *cis–trans* isomerization, the rate-determining step is the *cis–trans* isomerization whose barrier is about 22 kcal mol^{-1} in ethylene-promoted isomerization and 29 kcal mol^{-1} in the PH_3-promoted one. Thus, this Chalk–Harrod mechanism is more favorable than the modified Chalk–Harrod mechanism even if a *cis–trans* isomerization is involved in the reaction, but the barrier of the rate-determining step in the modified Chalk–Harrod mechanism is significantly lowered by the *cis–trans* isomerization; part of the $Pt(PH_3)_2$-catalyzed hydrosilylation of ethylene might occur through the modified Chalk–Harrod mechanism including the *cis–trans* isomerization.

Keywords: Hydrosilylation; Theoretical study; Reaction mechanism

1. Introduction

The transition-metal catalyzed hydrosilylation of an olefin is one of the most important synthetic reactions of organic silicon compounds [1]. Speier's catalyst, which consists of chloroplatinic acid in ethanol, is well known because of its significantly high catalytic activity [2]. Of course, not only Speier's catalyst but also many transition metal complexes have been applied to the hydrosilylation of alkene [1]. A widely accepted mechanism for the hydrosilylation of olefin is the Chalk–Harrod mechanism [3]. In this mechanism, the Si–H oxidative addition of silane to the transition metal complex occurs as the first step, and then, the olefin is inserted into M–H followed by the Si–C reductive elimination to release the product

(Scheme 1). Another mechanism was proposed later in the rhodium-catalyzed hydrosilylation of olefin, to interpret the observation of vinylsilane products [4–6]; in this mechanism, the olefin is inserted into M–SiR_3 followed by C–H reductive elimination (Scheme 1). Note that $M(H)(CH_2CH_2SiR_3)L_n$ is formed as an intermediate in this mechanism and its β-H abstraction yields vinylsilane. This is called the modified Chalk–Harrod mechanism. Many experimental results have been discussed based on these mechanisms.

Several variants in the reaction mechanism have been proposed for rhodium [7,8], iridium [9,10], zirconium [11], and samarium [12]. However, the first theoretical study should be undertaken on the above-mentioned Chalk–Harrod and modified Chalk–Harrod mechanisms, since these two reaction mechanisms are considered to be representative and most basic.

Although Speier's catalyst is very active [2], its active species is still ambiguous. Platinum bis-phosphine systems such as $Pt(C_2H_4)(PPh_3)_2$ [13a], $PtCl_2$[(*R*)-benzylmethylphenyl-phosphine]$_2$ [13b], $[Pt(\mu\text{-}H)(silyl)(PCy_3)]_2$ [14], and $Pt(PEt_2R)_2(C_2O_4)$ (R = alkyl chain bound to SiO_2) [15], have also been used as a catalyst in the hydrosilylation of olefin and acetylene. The platinum bis-phosphine complex seems more favourable for investigating its mechanism. Moreover, an interesting stereoselective hydrosilylation of olefin was carried out with Pt and Pd complexes of chiral phosphines such as (*R*)-benzylmethylphenylphosphine [13b] and (*S*)-2-diphenylphosphino-2′-methoxy-1,1′-binaphthyl [16]. Thus, it is worthwhile to investigate theoretically the Chalk–Harrod and modified Chalk–Harrod mechanisms in the hydrosilylation of ethylene catalyzed by a platinum bis-phosphine complex.

Recently, we investigated theoretically the reaction mechanism of the $Pt(PH_3)_2$-catalyzed hydrosilylation of ethylene [17]. The $TiCl_2$-catalyzed hydrosilylation reaction was theoretically investigated by Gordon et al. [18]. The purpose of this article is to present a detailed understanding of all the elementary steps involved in

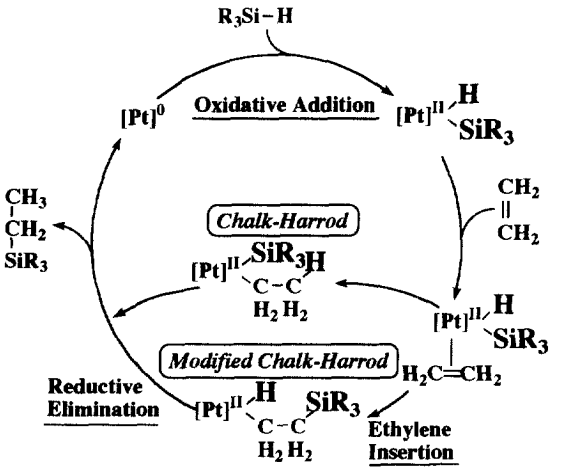

Scheme 1.

both the Chalk–Harrod and modified Chalk–Harrod mechanisms, to show what is the rate-determining step in $Pt(PH_3)_2$-catalyzed hydrosilylation of ethylene, and to elucidate which mechanism, Chalk–Harrod or modified Chalk–Harrod mechanism, is more favorable.

2. Model reactions examined

As shown in Scheme 1, the catalytic cycle consists of Si–H oxidative addition of silane to a Pt(0) complex, ethylene insertions into Pt–H and Pt–SiR_3, and Si–C and C–H reductive eliminations from Pt(II) complexes. Here, we adopted PH_3 as a model of tertiary phosphine such as PPh_3, PCy_3 etc., $HSiR_3$ (R = H, Cl, or Me) as a model of $HSiR'_3$ (R′ = Me, Et, Ph, Cl, OR etc.), and C_2H_4 as a model of stylene, 1-heptene, 1-octene etc [1–15]. A theoretical investigation was carried out on Si–H oxidative addition of $HSiR_3$ (R = H, Cl, or Me) to $Pt(PH_3)_2$ (Eq. (1)), formation of $PtH(SiR_3)(PH_3)(C_2H_4)$ (Eq. (2)), PH_3-ethylene exchange reaction to form $PtH(SiR_3)(PH_3)(C_2H_4)$ (Eq. (3)), ethylene insertion into either Pt–H or Pt–SiR_3 of $PtH(SiR_3)(PH_3)(C_2H_4)$ (Eqs. (3) and (4)), and C–H and Si–C reductive eliminations from platinum(II) hydride alkyl and platinum(II) alkyl silyl complexes (Eqs. (5) and (6)), respectively.

$$Pt(PH_3)_2 + HSiR_3 \rightarrow cis\text{-}PtH(SiR_3)(PH_3)_2 \quad (1)$$

$$cis\text{-}PtH(SiR_3)(PH_3)_2 + C_2H_4 \rightarrow cis\text{-}PtH(SiR_3)(PH_3)(C_2H_4) + PH_3 \quad (2)$$

$$cis\text{-}PtH(SiR_3)(PH_3)_2(C_2H_4) \rightarrow Pt(CH_2CH_3)(SiR_3)(PH_3) \quad (3)$$

$$cis\text{-}PtH(SiR_3)(PH_3)_2(C_2H_4) \rightarrow PtH(CH_2CH_3SiR_3)(PH_3) \quad (4)$$

$$cis\text{-}PtH(CH_3)(PH_3)L \rightarrow PtH(PH_3)L + CH_4 \quad (5)$$

$$cis\text{-}Pt(CH_3)(SiR_3)(PH_3)L \rightarrow Pt(PH_3)L + SiR_3CH_3 \quad (6)$$

(L = PH_3 or C_2H_4)

The term '*cis*' means that H and SiR_3 take a *cis*-position relative to each other in $PtH(SiR_3)(PH_3)_2$. In the other complexes, '*cis*' represents a similar meaning; for instance, H and $CH_2CH_2SiR_3$ take a *cis*-position to each other in $PtH(CH_2CH_2SiR_3)(PH_3)(C_2H_4)$.

Also, we present a brief explanation of the reasons why these model reactions are theoretically investigated here. Since Trogler et al. experimentally reported that the Pt(0) bis-phosphine complex without olefin undergoes the Si–H oxidative addition of silane [15], Eq. (1) was adopted here as a model reaction of the Si–H oxidative addition. Ethylene insertions into Pt–H and Pt–SiR_3 were investigated with a four coordinate complex, $PtH(SiR_3)(PH_3)(C_2H_4)$ (see Eqs. (3) and (4)). It was experimentally [19–21] and theoretically [22–24] reported that the ethylene insertion into metal-hydride occurs easily in a four-coordinate complex but occurs with difficulty in a five-coordinate complex when the central metal takes a d^8 electron configuration. To form $PtH(SiR_3)(PH_3)(C_2H_4)$, PH_3–C_2H_4 exchange must occur (Eq. (2)).

Two types of substitution reaction, associative substitution and dissociative one, are in general considered possible. Herein, these two reactions will be investigated. The ethylene insertion yields a three coordinate complex (see Eqs. (3) and (4)), to which either PH_3 or C_2H_4 coordinates to form $PtH(CH_2CH_2SiH_3)(PH_3)L$ and $Pt(CH_2CH_3)(SiH_3)(PH_3)L$ ($L = PH_3$ or C_2H_4) since a Pt(II) complex tends to take a four-coordinate planar structure. The C–H and Si–C reductive eliminations were investigated with model complexes, $PtH(CH_3)(PH_3)L$ and $Pt(CH_3)(SiR_3)(PH_3)L$, respectively, where CH_3 was employed as a model of CH_2CH_3 and $CH_2CH_2SiR_3$ (see Ref. [17] for the reliability of the model).

Though *cis*-$PtH(SiR_3)(PH_3)_2$ is directly produced by the Si–H oxidative addition to $Pt(PH_3)_2$, we should remember a possibility that this complex isomerizes to the *trans*-form. Our previous theoretical study clearly showed that ethylene is much more easily inserted into Pt–H and Pt–SiR_3 in *trans*-$PtH(SiR_3)(PH_3)(C_2H_4)$ than in the *cis*-form [25]. Since the high activation barrier of the ethylene insertion into Pt–SiR_3 is a reason that the modified Chalk–Harrod mechanism is difficult, as will be discussed below [17], one might expect that if *cis*-$PtH(SiR_3)(PH_3)_2$ easily isomerizes to the *trans*-form the modified Chalk–Harrod mechanism would become favorable. Thus, the reaction mechanism including the *cis–trans* isomerization (Eq. (7)) is worthy of theoretical investigation.

$$\textit{cis}\text{-}PtH(SiR_3)(PH_3)_2 \rightarrow \textit{trans}\text{-}Pt(SiR_3)(PH_3)_2 \tag{7}$$

This type of *cis–trans* isomerization is expected to occur through Berry's pseudo-rotation mechanism which needs coordination of the fifth ligand [26]. Actually, addition of a Lewis base induces the isomerization in a non-polar solvent [27]. PH_3 is one of the candidates, since PH_3 tends to eliminate from the Pt complex and free PH_3 would exist in the solution. C_2H_4 is the other candidate, since alkene exists in excess under the catalytic reaction conditions. Thus, we studied theoretically the PH_3- and C_2H_4-promoted *cis–trans* isomerizations of $PtH(SiH_3)(PH_3)_2$, where only the SiH_3 system was examined since the SiH_3 system gives a similar energy change to that of the $SiMe_3$ system (see below). Then, ethylene insertions into Pt–H and Pt–SiH_3 of *trans*-$PtH(SiH_3)(PH_3)(C_2H_4)$ were investigated theoretically (Eqs. (8) and (9)).

$$\textit{trans}\text{-}PtH(SiH_3)(PH_3)(C_2H_4) \rightarrow Pt(CH_2CH_3)(SiH_3)(PH_3) \tag{8}$$

$$\textit{trans}\text{-}PtH(SiH_3)(PH_3)(C_2H_4) \rightarrow PtH(CH_2CH_2SiH_3)(PH_3) \tag{9}$$

Since the products of Eqs. (8) and (9) are the same as the most stable products of Eqs. (3) and (4), respectively (vide infra), the succeeding C–H and Si–C reductive eliminations are the same as those of Eqs. (5) and (6), respectively.

3. Computations

Geometry optimization was carried out with the MP2 method in the Si–H oxidative addition to Pt(0) complex and the C–H and Si–C reductive eliminations

from Pt(II) complexes, since introduction of electron correlation effects considerably shifts the transition state to the Pt(0)-side [28]. Geometry changes in the *cis–trans* isomerization of $PtH(SiH_3)(PH_3)_2$ were also optimized with the MP2 method, since the five-coordinate intermediate and transition state were expected to be considerably influenced by correlation effects. However, geometry optimization was carried out at the SCF level in ethylene insertion reactions into Pt–H and $Pt–SiH_3$, since introduction of correlation effects does not shift the transition state very much [25]. All the transition states were determined so as to have only one negative eigenvalue of the Hessian matrix. In several cases, the transition state was further ascertained by calculating the vibrational frequencies.

Two types of basis set systems were adopted here. In the smaller system (BS-I), core electrons of Pt (up to 4f) and P (up to 2p) were replaced with effective core potentials (ECPs) [29,30], and their valence electrons were represented with (311/311/21) [29] and (21/21) [30] sets, respectively. For Si, C, and H atoms, MIDI-3 [31] and (31) [32] sets were employed, respectively. A d-polarization function [31] and a p-polarization function [32] were added to Si and an active H atoms, respectively, where the active H atom is a hydride and a hydrogen atom that changes into a hydride in the reaction. In the better basis set system (BS-II), the valence electrons of Pt and P were represented with (311/311/111) [29] and (21/21/1) [30] sets, respectively, with the same ECPs as those of BS-I, where a d-polarization function was added on P [31]. For Si and C, Huzinaga–Dunning (531111/4211/1) and (721/41/1) [32] sets were employed, respectively. A p-polarization function [32] was added to H except for H of PH_3. The BS-I was used for geometry optimization, while the BS-II was employed in MP4 and CCD calculations to estimate energy changes.

MP4 and CCD calculations were carried out with either MP2 or SCF-optimized geometries, where core electrons were excluded from the active space. In CCD calculations, the contribution of single and triple excitations was evaluated through fourth order perturbation using the CCD wavefunction [33]. This is named here CCD(ST4).

The Si–C reductive elimination was investigated with IRC calculation [34]. This calculation was performed with the MP2 method, in which the Hessian was calculated at each point of geometry change. Since this calculation is very time-consuming, only the Si–C reductive elimination was investigated with the IRC calculation. This is because the transition state of this reaction is non-planar against our expectation from orbital interaction diagram (wide infra). All these calculations were performed with Gaussian 94 program [35].

4. Formation of platinum(II) hydride silyl complex

4.1. Formation of cis-$PtH(SiR_3)(PH_3)_2$ through Si–H oxidative addition to $Pt(PH_3)_2$

Geometry changes in the Si–H oxidative addition of SiH_4 to $Pt(PH_3)_2$ are shown in Fig. 1 [36]. In the precursor complex, both $Pt(PH_3)_2$ and SiH_4 do not distort

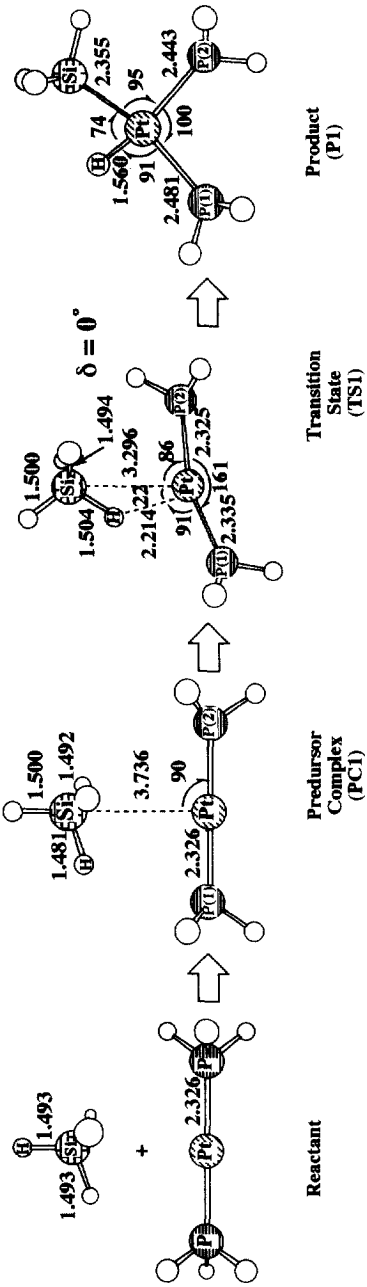

Fig. 1. Geometry changes in the Si–H oxidative addition of SiH_4 to $Pt(PH_3)_2$ (bond length in Å and bond angle in degree).

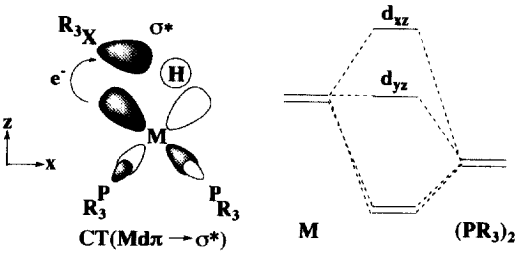

Scheme 2.

much and the Pt–SiH_4 distance is very long. These features suggest that the interaction between $Pt(PH_3)_2$ and SiH_4 is very weak and the precursor complex might be considered a van der Waals complex. In the transition state (TS), the Si–H bond to be broken in the reaction lengthens only slightly, the P–Pt–P angle is not closed very much, and the Pt–H and Pt–Si distances are still very long. From these geometrical features, the transition state is considered reactant-like. It is noted that this transition state is planar. This is easily interpreted in terms of the charge-transfer interaction between Pt d and Si–H σ* orbitals. In the oxidative addition reaction, the charge-transfer from the metal d orbital to the σ* orbital must occur to break the bond and to form M–H and M–SiR_3 bonds [37]. Because the Pt d_{xz} orbital is destabilized in energy by anti-bonding overlap with PH_3 lone pair orbital (Scheme 2) [38], a strong charge-transfer interaction is formed when the Si–H σ* orbital can interact with the Pt d_{xz} orbital. The Si–H σ* orbital interacts with the Pt d_{xz} orbital in the planar TS, but cannot in the non-planar TS. Thus, the planar TS is more favorable than the non-planar TS.

The product, *cis*-$PtH(SiH_3)(PH_3)_2$, takes a planar four-coordinate structure. Interestingly, the Pt–PH_3 bond *trans* to SiH_3 is longer than the Pt–PH_3 bond *trans* to H (hydride). This clearly indicates that SiH_3 has stronger *trans*-influence than H (hydride). The strong *trans*-influence of silyl group was also experimentally reported by Chatt et al. [39].

Binding energy (BE), activation barrier (E_a), and reaction energy (ΔE) were calculated with various computational methods, as shown in Table 1, where BE is an energy difference between the precursor complex and the sum of reactants, E_a is an energy difference between the precursor complex and TS, and ΔE is an energy difference between the product and the sum of reactants. Their negative values represent the stabilization in energy. As expected, introduction of electron correlation significantly decreases E_a and increases BE and exothermicity E_{exo}. The BE value is very small in all the reaction systems, which is consistent with the idea that the precursor complex is a van der Waals complex. E_a slightly fluctuates around the MP2 and MP3 levels, but fluctuates much less upon going to CCD(ST4) from MP4SDQ. In particular, E_a of the MP4SDQ level is almost the same as that of the CCD(ST4) level. The instability of the Hartree–Fock wave function was not observed at the TS.

From these results, the energy changes calculated with the MP4SDQ method are considered reliable. Interestingly, E_a depends little on the substituent of the Si atom (Table 1). This is because the TS is reactant-like. On the other hand, ΔE significantly depends on the substituent, which is consistent with the fact that the Pt–silyl bond is stabilized by introduction of an electron-withdrawing substituent.

4.2. Formation of trans-$PtH(SiH_3)(PH_3)L$ ($L = PH_3$ or C_2H_4) through cis–trans isomerization of $PtH(SiH_3)(PH_3)_2$

PH_3- and C_2H_4-promoted *cis–trans* isomerization of $PtH(SiH_3)(PH_3)_2$ was theoretically investigated here [40]. In Fig. 2 [40], geometry changes of C_2H_4-promoted *cis–trans* isomerization are shown. Ethylene coordination yields a distorted square pyramidal complex **SP5** and a trigonal bipyramidal complex **TBP5a**. The latter is slightly more stable than the former by only 2.5 kcal mol^{-1} (hereafter, energy values calculated with MP4SDQ/BS II are provided without any notice since the MP4SDQ/BS II calculation gives almost the same energy change as the better method, as discussed here and above). The transition state **TS5a** is considered to be a trigonal bipyramidal structure in which C_2H_4, H, and SiH_3 are in an equatorial plane but two PH_3 ligands take an axial position. If the transition state was optimized under the assumption that C_2H_4 was placed to be parallel to the Pt–SiH_3

Table 1
The binding energy (BE)[a], activation energy (E_a)[b], and reaction energy (ΔE)[c] of the Si–H oxidative addition of $HSiR_3$ to $Pt(PH_3)_2$ (kcal mol^{-1})

	BE[a]	E_a[b]	ΔE[c]
R = H			
HF	0.5	8.3	−6.4
MP2	−2.3	2.0	−24.2
MP3	−2.1	4.3	−21.7
MP4DQ	−2.0	0.6	−21.9
MP4SDQ	−2.3	2.4	−21.9
SD-CI(DS)[d]	–	1.2	−22.7
SD-CI(P)[e]	–	0.9	−21.1
CCD(ST4)	−2.5	2.8	−21.7
R = Me			
MP4SDQ	−3.7	3.0	−16.8
R = Cl			
MP4SDQ	−4.9	2.8	−32.3

[a] BE, an energy difference between the precursor complex and the sum of reactants.
[b] E_a, an energy difference between the precursor complex and TS.
[c] ΔE, an energy difference between the product and the sum of reactants.
[d] Davidson–Silver correction for higher-order excited configurations (E.R. Davidson, D.W. Silver, Chem. Phys. Lett. 52 (1977) 403).
[e] Pople correction for higher-order excited configurations (J.A. Pople, R. Seeger, R. Krishnan, Int. J. Quant. Chem. 11 (1977) 149).

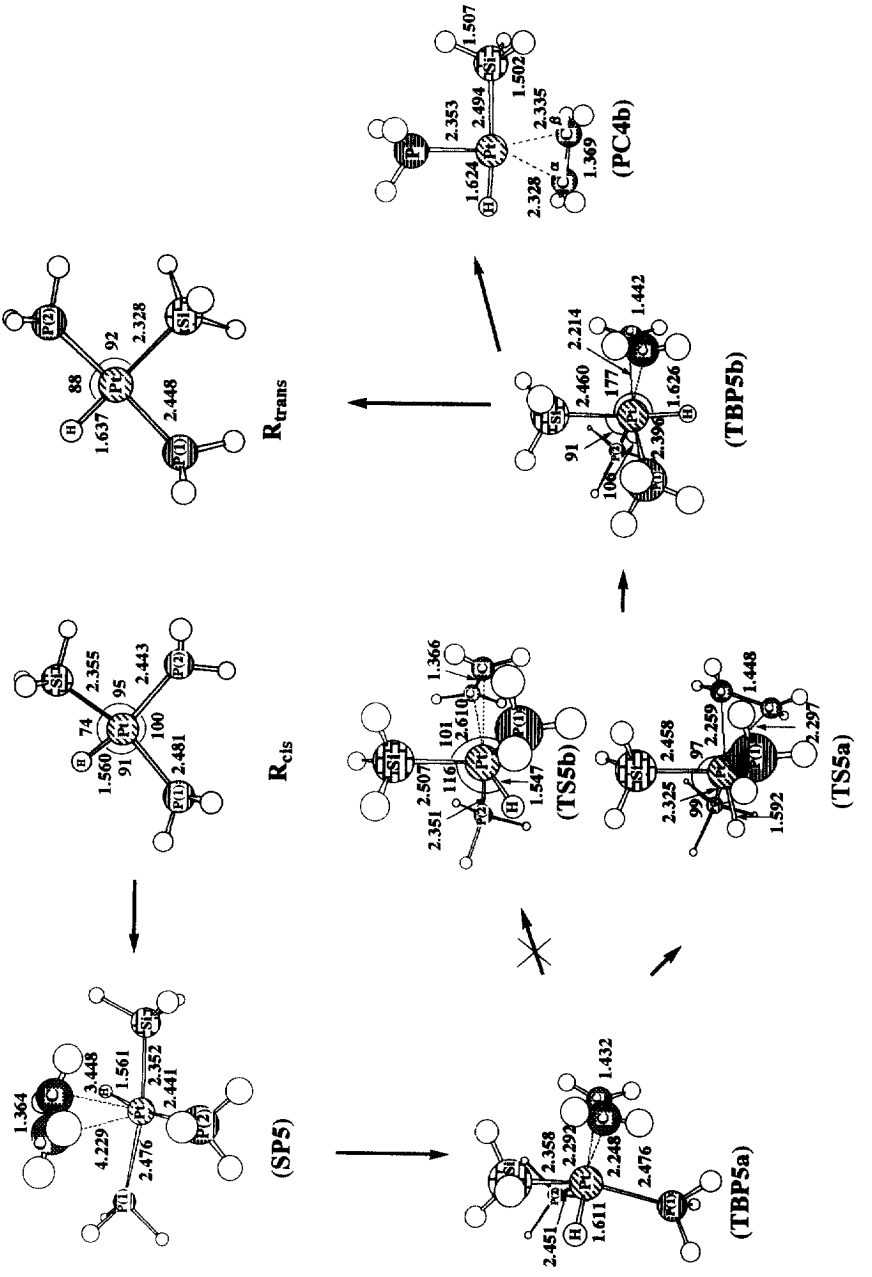

Fig. 2. Geometry changes of C_2H_4-promoted *cis–trans* isomerization of $PtH(SiH_3)(PH_3)_2$ (bond length in Å and bond angle in degree).

bond, i.e. to be perpendicular to the equatorial plane, **TS5b** was obtained. This **TS5b** is less stable than **TS5a** by ca. 17 kcal mol^{-1}. As is well known, an electron-withdrawing ligand prefers the equatorial position to the axial position, to form the π-back donating interaction [41]. In **TS5a**, C_2H_4 takes the equatorial position and can form the π-back donating interaction with the d orbital that is destabilized in energy by the other two equatorial ligands, H and SiH_3. In **TS5b**, C_2H_4 is in the equatorial plane but cannot form the π-back donating interaction with the equatorial d orbital. This is the reason that **TS5a** is more stable than **TS5b**. The movement of H to the position *trans* to SiH_3 leads to a different trigonal bipyramidal structure **TBP5b**. If one PH_3 eliminates from **TBP5b**, *trans*-$PtH(SiH_3)(PH_3)(C_2H_4)$ is produced, from which ethylene insertion takes place, as will be discussed below in more detail. Geometry changes of PH_3-promoted isomerization are omitted here to save the space, since the PH_3-promoted isomerization is less important (see below).

The C_2H_4-promoted isomerization occurs with a lower barrier (22.1 kcal mol^{-1}) than the PH_3-promoted isomerization ($E_a = 28.5$ kcal mol^{-1}). Why does the PH_3-promoted isomerization need a higher E_a value than the C_2H_4-promoted isomerization? We can easily find the reason by inspecting the geometry and interaction of the TS. In **TS5a**, the C_2H_4 π* orbital can overlap well with the equatorial d orbital that is destabilized by strong H (hydride) and SiH_3 ligands, since C_2H_4 is in the equatorial plane. On the other hand, PH_3 cannot form the π-back donating interaction with the equatorial d orbital, since PH_3 does not have a good acceptor orbital unlike C_2H_4. As a result, the PH_3-promoted isomerization needs a much higher activation energy than the C_2H_4-promoted isomerization. A similar discussion based on the π-back donation between Pt dπ and C_2H_4 π* orbitals was presented above to explain the lower stability of **TS2b** than that of **TS2a**. We mention here the reaction energy ΔE. Though the *trans*-complex is about 10 kcal mol^{-1} less stable than the *cis*-complex, **TBP5b** in the product-side is slightly less stable by only 1.3 kcal mol^{-1} than **TBP5a** in the reactant-side. Thus, the *cis-trans* isomerization might occur, whereas the *trans*-complex is less stable than the *cis*-form.

5. Formation of platinum(II) hydride silyl ethylene complex

There are two possible reaction courses to form a four coordinate complex, $PtH(SiR_3)(PH_3)(C_2H_4)$ from $PtH(SiR_3)(PH_3)_2$ through PH_3–C_2H_4 exchange. One is an associative process which occurs through C_2H_4 coordination to Pt followed by PH_3 elimination (Eq. (10)), and the other is a dissociative process which occurs through PH_3 elimination followed by C_2H_4 coordination (Eq. (11)). In the associa-

$$PtH(SiR_3)(PH_3)_2 \xrightarrow{+C_2H_4} PtH(SiR_3)(PH_3)_2(C_2H_4) \xrightarrow{-PH_3} PtH(SiR_3)(PH_3)(C_2H_4) \quad (10)$$

$$PtH(SiR_3)(PH_3)_2 \xrightarrow{-PH_3} PtH(SiR_3)(PH_3) \xrightarrow{+C_2H_4} PtH(SiR_3)(PH_3)(C_2H_4) \quad (11)$$

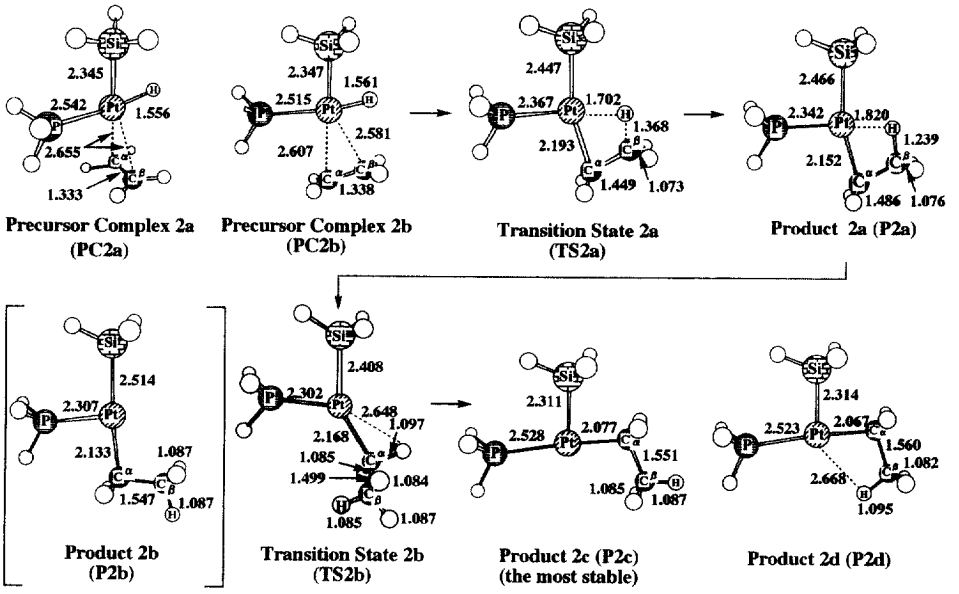

Fig. 3. Geometry changes in the ethylene insertion into the Pt–H bond of *cis*-$PtH(SiH_3)(PH_3)(C_2H_4)$ (bond length in Å and bond angle in degree).

tive process, the C_2H_4 coordination to $PtH(SiH_3)(PH_3)_2$ **P1** yields $PtH(SiH_3)(PH_3)_2(C_2H_4)$ **SP5** and **TBP5a** (Fig. 2) with energy stabilization of 2.5 and 5.0 kcal mol^{-1}, respectively. In **SP5**, $PH_3(1)$ elimination yields **PC2b** (Fig. 3) with energy destabilization of 8.7 kcal mol^{-1}, and $PH_3(2)$ elimination yields **PC3b** (Fig. 4) with an energy destabilization of 8.8 kcal mol^{-1}. $PH_3(2)$ elimination from **TBP5a** yields *cis*-$PtH(SiH_3)(PH_3)(C_2H_4)$ **PC3b** (Fig. 4) with energy destabilization of 11.3 kcal mol^{-1} (note that **PC2b**, **PC3b**, and **PC4b**, in which C_2H_4 is in the molecular plane, are more stable than **PC2a**, **PC3a**, and **PC4a**, in which C_2H_4 is perpendicular to the molecular plane, as will be discussed below). The similar associative substitution reaction of d^8 transition metal complexes was investigated theoretically by Hall et al. [42]. In their work, the substitution occurs via a trigonal bipyramidal transition state with a small barrier of 2–7 kcal mol^{-1} for NH_3–NH_3 exchange in Pt(II) complexes. In our work **SP5** and **TBP5a** are intermediates. This is probably because ethylene coordination would stabilize five coordinate complexes and PH_3 is more soft than NH_3 (we failed to find the transition state by changing bond angle and Pt–PH_3 bond distance in **SP5**, **TBP5a**, and **TBP5b**). Considering the low activation barrier in their work and the existence of **SP5** and **TBP5a** in our work, the formation process of $PtH(SiR_3)(PH_3)(C_2H_4)$ would not require a higher activation barrier than the rate-determining step of this catalytic cycle (see below).

In the dissociative process, PH_3 which is in a position *trans* to SiH_3 eliminates from **P1** to yield a three coordinate complex, $PtH(SiH_3)(PH_3)$, with energy destabilization of 23.9 kcal mol^{-1} [25], and C_2H_4 coordination to $PtH(SiH_3)(PH_3)$ yields *cis*-$PtH(SiH_3)(PH_3)(C_2H_4)$ **PC2b** with energy stabilization of 17.7 kcal mol^{-1}. The

different PH_3 which is in a position *trans* to H eliminates from **P1** with energy destabilization of 31.9 kcal mol^{-1}. C_2H_4 coordination to this complex yields **PC3b** with energy stabilization of 25.8 kcal mol^{-1}. Apparently, the dissociative process causes larger energy destabilization than the associative process.

The formation of *trans*-$PtH(SiH_3)(PH_3)(C_2H_4)$ **PC4b** (Fig. 4) was also investigated, taking into consideration both the associative and dissociative processes. In the associative process, C_2H_4 coordination occurs first, followed by the *cis–trans* isomerization to form **TBP5b** with an activation barrier of 23 kcal mol^{-1} (vice supra). PH_3 elimination from **TBP5b** gives rise to energy destabilization of 14.0 kcal mol^{-1}, to form **PC4b**. This energy destabilization is smaller than the activation barrier of the *cis–trans* isomerization. In the dissociative process, PH_3 dissociates from **P1** to form a three coordinate complex *cis*-$PtH(SiH_3)(PH_3)$ with energy destabilization of 24.6 kcal mol^{-1} [25]. This complex must isomerize to the *trans*-form followed by C_2H_4 coordination. The isomerization needs an activation barrier of 31.7 kcal mol^{-1}. Again, the dissociative process causes the much greater energy destabilization.

In conclusion, the associative process occurs more easily than the dissociative process to form both *cis*- and *trans*-$PtH(SiH_3)(PH_3)(C_2H_4)$. Thus, it is reasonably concluded that the PH_3–C_2H_4 exchange occurs through the five-coordinate intermediates, **SP5**, **TBP5a**, and **TBP5b**; the PH_3 elimination to form **PC2b**, **PC3b**, and **PC4b** needs energy destabilization of 9–11 kcal mol^{-1} which is lower than the barrier of the rate-determining step of the catalytic cycle, as will be discussed below. Though this estimate was not carried out for R = Cl and Me, similar energy changes would occur.

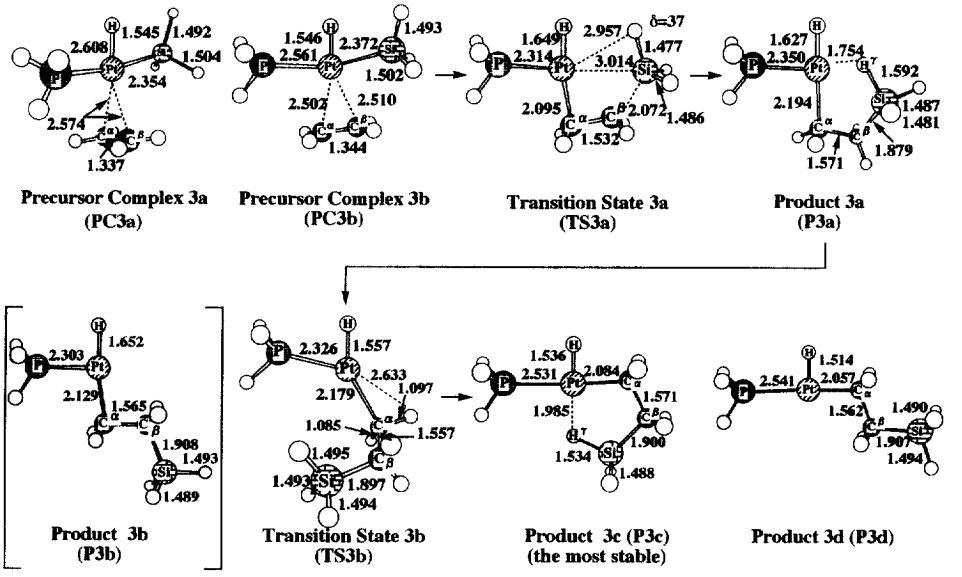

Fig. 4. Geometry changes in the ethylene insertion into the Pt–SiH_3 bond of *cis*-$PtH(SiH_3)(PH_3)(C_2H_4)$ (bond length in Å and bond angle in degree).

6. Ethylene insertion into either Pt–H or Pt–SiR_3 of $PtH(SiR_3)(PH_3)(C_2H_4)$

6.1. Insertion into Pt–H of cis-$PtH(SiR_3)(PH_3)(C_2H_4)$

Two structures of *cis*-$PtH(SiH_3)(PH_3)(C_2H_4)$ are shown in Fig. 3. In one structure (**PC2a**), ethylene is perpendicular to the molecular plane while in the other (**PC2b**) ethylene is in the molecular plane. The latter is slightly more stable than the former, while the energy difference between them is only 2.7 kcal mol^{-1}. In the transition state (**TS2a**), the Pt–C^{α} distance is 2.193 Å, which is almost the same as the Pt–alkyl bond distance in the product. On the other hand, the Pt–H distance is still short (1.702 Å), only 0.14 Å longer than those of **PC2a** and **PC2b**. Consistent with this short Pt–H distance, the C^{α}–H distance (1.37 Å) is much longer than the usual C–H bond. From these geometrical features, the transition state might be characterized as follows: the Pt–alkyl bond has already been formed, while the C–H bond formation is on the way and the Pt–H bond still remains.

In the product just after the insertion (**P2a**), the Pt–H distance is 1.82 Å and the C^{α}–H distance is 1.24 Å, which is much longer than the usual sp^3 C–H bond. These geometric features clearly show that **P2a** involves an agostic interaction. The strength of the agostic interaction is estimated as an energy difference between **P2a** and **P2b**, since an agostic interaction is not involved in **P2b** but the positions of the other ligands in **P2b** are the same as those of **P2a**. The difference is about 14 kcal mol^{-1}, indicating that the agostic interaction is fairly strong. However, **P2a** is not the most stable in spite of the strong agostic interaction. This is because two strong silyl and alkyl ligands take positions *trans* to each other (remember that the *trans*-influence of silyl ligand is very strong). The most stable product is **P2c**, because the position *trans* to the silyl ligand is empty. Isomerization from **P2a** to **P2c** proceeds through the transition state **TS2b**. In **TS2b**, the Pt–H distance lengthens to 2.65 Å, indicating that the agostic interaction is broken. The alkyl group, which is moving to the position *trans* to PH_3, overlaps well with the Pt doubly occupied d orbital. Therefore, the origin of the barrier is attributable to the breaking of agostic interaction and the four-electron repulsion between alkyl lone pair and Pt doubly occupied d orbitals.

The activation barriers for the ethylene insertion E_a(TS2a) and the isomerization of ethylene insertion product E_a(TS2b) are calculated with HF, MP2-MP4SDQ, SD-CI and CCD(ST4) methods, as listed in Table 2, where E_a(TS2a) is an energy difference between **PC2b** and **TS2a** and E_a(TS2b) is an energy difference between **PC2b** and **TS2b** (since **P2a** is only slightly more stable than **TS2a**, **P2a** is not considered a stable intermediate, and therefore, the activation barrier for the isomerization should be taken as an energy difference between **TS2b** and **PC2b**). ΔE is an energy difference between the most stable product and **PC2b**. Introduction of electron correlation effects decreases E_a(TS2a) and E_a(TS2b) to a lesser extent than E_a of the Si–H oxidative addition (see Table 1). Moreover, E_a(TS2a) and E_a(TS2b) fluctuate little upon going to CCD(ST4) from MP2. These results show that electron correlation effects are indispensable for a quantitative estimate of energy change but much less important than those in the oxidative addition and reductive

Table 2
Activation energy (E_a) and reaction energy (ΔE) of the ethylene insertion into Pt–H and Pt–SiH_3 bonds (kcal mol^{-1})

(A) Insertion reactions of *cis*-$PtH(SiH_3)(PH_3)(C_2H_4)$

	Insertion into Pt–H			Insertion into Pt–SiH_3		
	E_a(TS2a)[a]	E_a(TS2b)[a]	ΔE[b]	E_a(TS3a)[a]	E_a(TS3b)[c]	ΔE[b]
HF	15.6	26.2	−6.7	44.1	15.4	8.6
MP2	9.9	22.7	−5.7	42.8	18.9	10.3
MP3	11.9	22.9	−8.3	41.3	17.0	5.5
MP4DQ	12.6	22.6	−7.2	43.7	20.0	8.0
MP4SDQ	12.7	22.4	−6.7	44.1	20.5	9.0
SD-CI(DS)	12.0	22.4	−7.4	–	–	–
SD-CI(P)	12.0	22.4	−7.4	–	–	–
CCD(ST4)	12.2	22.5	−6.7	–	–	–

(B) *Insertion reactions of trans-*$PtH(SiH_3)(PH_3)(C_2H_4)$

	Insertion into Pt–H		Insertion into Pt–SiH_3	
	E_a(TS6a)[a]	ΔE[b]	E_a(TS6b)[a]	ΔE[b]
MP4SDQ	3.6	−17.4	15.9	−2.5

[a] E_a, an energy difference between the most stable precursor complex and the transition state.
[b] ΔE, an energy difference between the product and the most stable precursor complex.
[c] E_a, an energy difference between **TS3b** and **P3a**.

elimination. E_a(TS2a) of 12–13 kcal mol^{-1} seems moderate, but E_a(TS2b) is much higher than E_a(TS2a) (see Table 2), indicating that the real transition state to reach the most stable product is **TS2b**, and the reaction needs activation energy of 23 kcal mol^{-1}, when R = H.

The ethylene insertion into Pt–H of *cis*-$PtH(SiR_3)(PH_3)(C_2H_4)$ (R = Cl or Me) was also investigated (geometry changes are omitted here). E_a(TS2b) was calculated to be 25.7 kcal mol^{-1} for R = Cl and 22.6 kcal mol^{-1} for R = Me. Interestingly, the E_a(TS2b) difference between R = H and Me is only 3 kcal mol^{-1}.

6.2. Insertion into $Pt–SiR_3$ of *cis*-$PtH(SiR_3)(PH_3)(C_2H_4)$

Geometry changes for R = H are shown in Fig. 4. The ethylene complex, **PC3b**, in which ethylene is in the molecular plane, is slightly more stable than **PC3a** in which ethylene is perpendicular to the molecular plane. In the transition state **TS3a**, the Pt–C^{α} distance is 2.095 Å, which is almost the same as that of the product. The Pt–Si distance of 3.01 Å is much longer than that of the reactant (**PC3a** and **PC3b**), and the Si–C^{β} distance of 2.07 Å is only 0.17 Å longer than that of the product. These geometric features indicate that the Pt–alkyl and Si–C^{β} bonds are almost formed and the Pt–silyl bond is almost broken at the transition state. In other words, this transition state is product-like.

In the product **P3a** just after the insertion, the Pt–H^{γ} distance is 1.75 Å, which is only 0.2 Å longer than the usual Pt–hydride bond. The Si–H bond which takes the nearest position to Pt is longer than the usual Si–H bond by ca. 0.1 Å. These geometric features again indicate that **P3a** involves an agostic interaction between Pt and H^{γ}. The strength of the agostic interaction is estimated as an energy difference between **P3a** and **P3b** in which the agostic interaction disappears but all the ligands take the same positions as those of **P3a**. This energy difference is about 18 kcal mol^{-1}, which is slightly stronger than the agostic interaction of **P2a** probably because H of SiH_3 is more negatively charged than H of CH_3 and might be able to form a stronger charge-transfer interaction. Remember the theoretical report [43] that the agostic interaction is formed through the charge-transfer interaction from X–H σ orbital (X = C, Si etc.) to the metal unoccupied d orbital. In spite of this fairly strong agostic interaction, **P3a** is not the most stable, because two strong hydride and alkyl ligands take positions *trans* to each others. The most stable product is **P3c**, since the position *trans* to hydride is empty. A weak agostic interaction is formed between Pt and H^{γ} in **P3c**. **P3d** is slightly less stable than **P3c** because of the lack of the agostic interaction. Isomerization from **P3a** to **P3c** occurs through the transition state **TS3b**. In **TS3b**, again the agostic interaction disappears and the alkyl sp^3 lone pair orbital overlaps well with Pt doubly occupied d orbital, like **TS2b**. We mention here **P3d** which is a rotation isomer of **P3c**. Though **P3d** exists as a local minimum, the geometry of **TS3b** suggests that **P3c** is formed directly from **TS3b** since SiH_3 takes a position near to Pt in **TS3b**.

The activation barrier and reaction energy are listed in Table 2. E_a(TS3a) is defined as an energy difference between **PC3a** and **TS3a**. E_a(TS3b) is defined as an energy difference between **TS3b** and **P3a**, since **P3a** can be viewed as a stable intermediate unlike **P2a** (note that **P3a** is much more stable than **TS3a**). Both E_a(TS3a) and E_a(TS3b) only fluctuate slightly upon going to MP4SDQ from MP2. It is important that E_a(TS3a) is much larger than E_a(TS2b), indicating that the ethylene insertion into Pt–SiH_3 occurs with much more difficulty than does the insertion into Pt–H.

It is worthwhile investigating the reason why the ethylene insertion into Pt–SiH_3 needs a much higher activation energy than the insertion into Pt–H. We examined the reason from two points of view. One is the reaction energy which is related to the thermodynamic point of view. The Pt–H bond is broken and the C–H bond is formed in the ethylene insertion into Pt–H. In the insertion into Pt–SiH_3, the Pt–SiH_3 bond is broken and the C–Si bond is formed. In both insertion reactions, the C=C double bond changes into a C–C single bond and the Pt–alkyl bond is newly formed. Since these bond changes would not be substantially affected by the SiH_3 substituent, we do not take into consideration these bond changes, but examine here differences between Pt–H and Pt–SiH_3 bonds and between C–H and C–Si bonds. Though the Pt–H bond (59 kcal mol^{-1}) is as strong as the Pt–SiH_3 bond (54 kcal mol^{-1}), the C–H bond (109 kcal mol^{-1}) is much stronger than the C–Si bond (87 kcal mol^{-1}), where in parentheses are MP4SDQ-calculated bond energies in *cis*-$PtH(SiH_3)(PH_3)_2$, CH_4, and CH_3SiH_3. This means that the ethylene insertion into Pt–H yields a greater stabilization energy than the insertion into Pt–H, which favors the ethylene insertion into Pt–H.

The other point of view is an interaction at the transition state. Since the H (hydride) 1s valence orbital is spherical, the hydride can start to form a new C–H bond without significant weakening of the Pt–H bond. On the other hand, SiH_3 must change its orientation toward ethylene to form a new C–Si bond, since the valence orbital of SiH_3 is a directional sp^3 orbital (Scheme 3) [25,44]. This orientation change of SiH_3 significantly weakens the Pt–SiH_3 bond. In other words, the Pt–SiH_3 bond must be broken to form the new Si–C bond. This means that the energy destabilization takes place in the ethylene insertion into Pt–SiH_3. This explanation was successfully supported by the fact that the insertion into Pt–SiH_3 yields a much larger distortion energy of $PtH(SiH_3)(PH_3)$ (41.4 kcal mol^{-1}) than does the insertion into Pt–H (7.4 kcal mol^{-1}) and the larger distortion energy of the former insertion arises mainly from the Pt–SiH_3 bond weakening, where the distortion energy of $PtH(SiR_3)(PH_3)$ is defined as an energy difference between the equilibrium structure and the distorted one taken at the TS. A similar discussion was presented to explain the difference between C–H and C–C oxidative additions [45–47]. From these results, it is reasonably concluded that the ethylene insertion into Pt–SiR_3 occurs with more difficulty than that into Pt–H because of the lower stability of the product and the highly directional sp^3 valence orbital of SiR_3.

6.3. Insertion into Pt–H and Pt–SiH_3 in trans-$PtH(SiH_3)(PH_3)(C_2H_4)$

Geometry changes of the ethylene insertion into Pt–H and Pt–SiH_3 of *trans*-$PtH(SiH_3)(PH_3)(C_2H_4)$ are shown in Fig. 5 [40]. The transition state structures of these insertion reactions are essentially the same as those of the insertions in the *cis*-complex, while the transition states of the *trans*-complex somewhat shift to the reactant-side; for instance, the Pt–H distance is shorter and the C^{β}–H distance is longer in **TS4a** than those in **TS2a** of the insertion of *cis*-$PtH(SiH_3)(PH_3)(C_2H_4)$. Similar differences are observed between **TS4b** and **TS3a**.

One of the significant differences in the ethylene insertion reaction between *cis*- and *trans*-$PtH(SiH_3)(PH_3)(C_2H_4)$ is that the ethylene insertion product of the *trans*-complex does not need to cause isomerization but the ethylene insertion product of the *cis*-complex must cause isomerization, as follows. In the insertion into Pt–H of the *trans*-complex, the alkyl group is formed at a position *trans* to

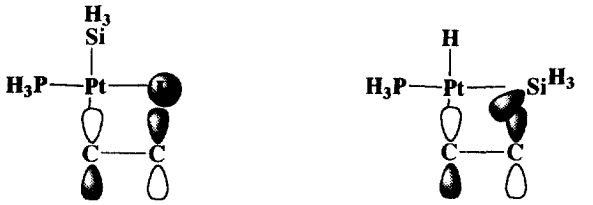

C_2H_4 Insertion into Pt-H **C_2H_4 Insertion into Pt-SiH_3**

Orbital Interaction

Scheme 3.

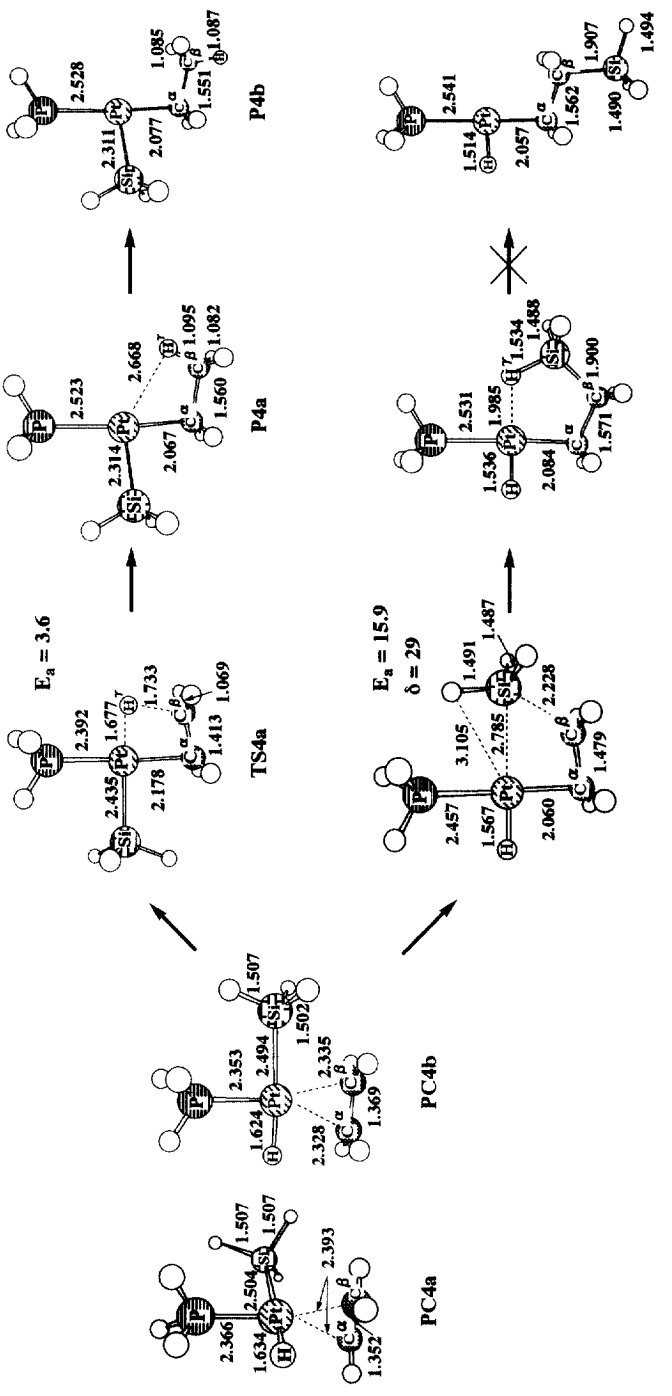

Fig. 5. Geometry changes in the ethylene insertion into Pt–H and Pt–SiH_3 bonds of *trans*-$PtH(SiH_3)(PH_3)(C_2H_4)$ (bond length in Å and bond angle in degree).

PH_3, and SiH_3 and alkyl take positions *cis* to each other (see **P4a**). In the insertion into Pt–SiH_3 of the *trans*-complex, the alkyl group is also formed at the position *trans* to **PH3**, and H and alkyl take positions *cis* to each other (see **P4c**). Thus, the insertion products are stable and do not need to isomerize.

The activation barrier (E_a) and reaction energy (ΔE) are shown in Table 2. Important results are summarized as follows: (1) E_a of the insertion into Pt–H is much lower than that of the insertion into Pt–SiH_3. This is common in both *cis*- and *trans*-complexes. (2) E_a values of both insertions into Pt–H and Pt–SiH_3 are much lower in the *trans*-complex than those in the *cis*-complex. Apparently, the ethylene insertion occurs much more easily in the *trans*-complex than in the *cis*-complex.

The reason for the easy insertion of the *trans*-complex is understood in terms of the *trans*-influence. Pt–H and Pt–SiH_3 bonds of the *trans*-complex are weaker than those of the *cis*-complex, since these bonds take a position *trans* to each other in the *trans*-complex (remember that *trans*-influence of SiH_3 is stronger than *trans*-influence of PH_3, as discussed above). Actually, Pt–H and Pt–SiH_3 bonds of the *trans*-complex are longer than those of the *cis*-complex by ca. 0.07 and 0.15 Å, respectively. This means that the insertion in the *trans*-complex occurs more easily than that in the *cis*-complex. The other reason is the stability of transition state. In the transition state, the Pt–alkyl bond is almost formed. In the insertion of the *trans*-complex, the Pt–alkyl bond is formed at the position *trans* to PH_3, while in the insertion of the *cis*-complex, the Pt–alkyl bond is formed at the position *trans* to either H or SiH_3. Since the *trans*-influence of PH_3 is much weaker than that of H and SiH_3, the Pt–alkyl bond is more stable at the TS of the *trans*-complex than that of the *cis*-complex. This leads to the lower barrier of the insertion in the *trans*-complex.

7. C–H and Si–C reductive elimination from Pt(II) complexes

The C–H and Si–C reductive eliminations were investigated in detail in $PtH(CH_3)(PH_3)_2$ and $Pt(CH_3)(SiH_3)(PH_3)_2$. Those transition state structures exhibit interesting differences, as shown in Fig. 6. In the TS of the C–H reductive elimination, the C–H distance is 1.457 Å and the Pt–H and Pt–C distances are 1.606 and 2.268 Å, respectively (Fig. 6(A)). These features indicate that this transition state is much more on the Pt(II)-side than the TS of the Si–H oxidative addition. It is also important that this TS is planar. On the other hand, the TS of Si–C reductive elimination is non-planar in which the dihedral angle between $Pt(PH_3)_2$ and Pt(Si–C) planes is 70° (Fig. 6(B)). This non-planar TS is in contrast to our expectation from an orbital interaction diagram; the orbital interaction diagram suggests that the planar TS is more stable than the non-planar TS, as discussed above (see also Scheme 2). The reactant $Pt(CH_3)(SiH_3)(PH_3)_2$ is planar and a singlet, as expected. $Pt(PH_3)_2$ is also a singlet. Thus, the non-planar TS should be connected to the planar reactant on the singlet surface. To ascertain this feature, we carried out an intrinsic reaction coordinate (IRC) calculation. As shown

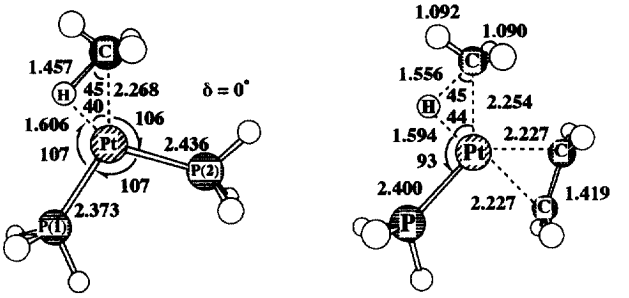

(A) C-H reductive elimination from cis-PtH(CH_3)(PH_3)L (L = PH_3 or C_2H_4)

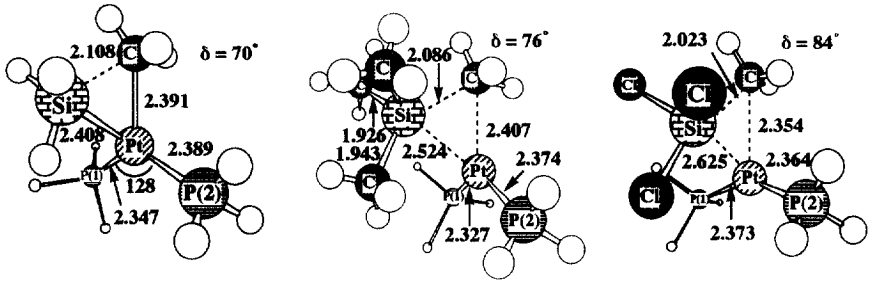

(B) Si-C reductive elimination of cis-Pt(SiR_3)(CH_3)(PH_3)$_2$

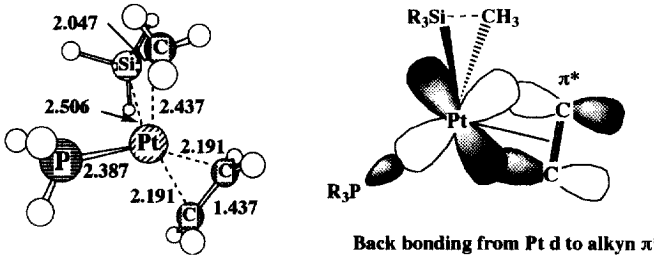

Back bonding from Pt d to alkyn π*

(C) Si-C reductive elimination of cis-Pt(SiR_3)(CH_3)(PH_3)(C_2H_4)

Fig. 6. Transition states of C–H and Si–C reductive elimination of *cis*-PtH(CH_3)(PH_3)L (L = PH_3 or C_2H_4) (bond length in Å and bond angle in degree).

in Fig. 7, the dihedral angle of 70° gradually decreases upon going to the reactant from the TS [36]. When the Si–C distance is shorter than 2.6 Å, the dihedral angle still remains at about 70°. When the Si–C distance becomes longer than 2.6 Å, the dihedral angle starts to decrease gradually to 0°. The triplet state is over 100 kcal mol^{-1} more unstable than the singlet state at the TS (UMP2/BS-I calculation). These results clearly show that the planar reactant is smoothly connected to the non-planar TS on the singlet surface.

The Pt dπ orbital population (1.830e) in the planar transition state is less than that (1.911e) in the non-planar transition state, where the numbers in parentheses are calculated for the Si–C reductive elimination of $Pt(CH_3)(SiH_3)(PH_3)_2$. This electron distribution indicates that the charge-transfer interaction from Pt d to the Si–C σ* orbital is stronger in the planar transition state than in the non-planar state. This is consistent with expectation from the orbital interaction diagram. The

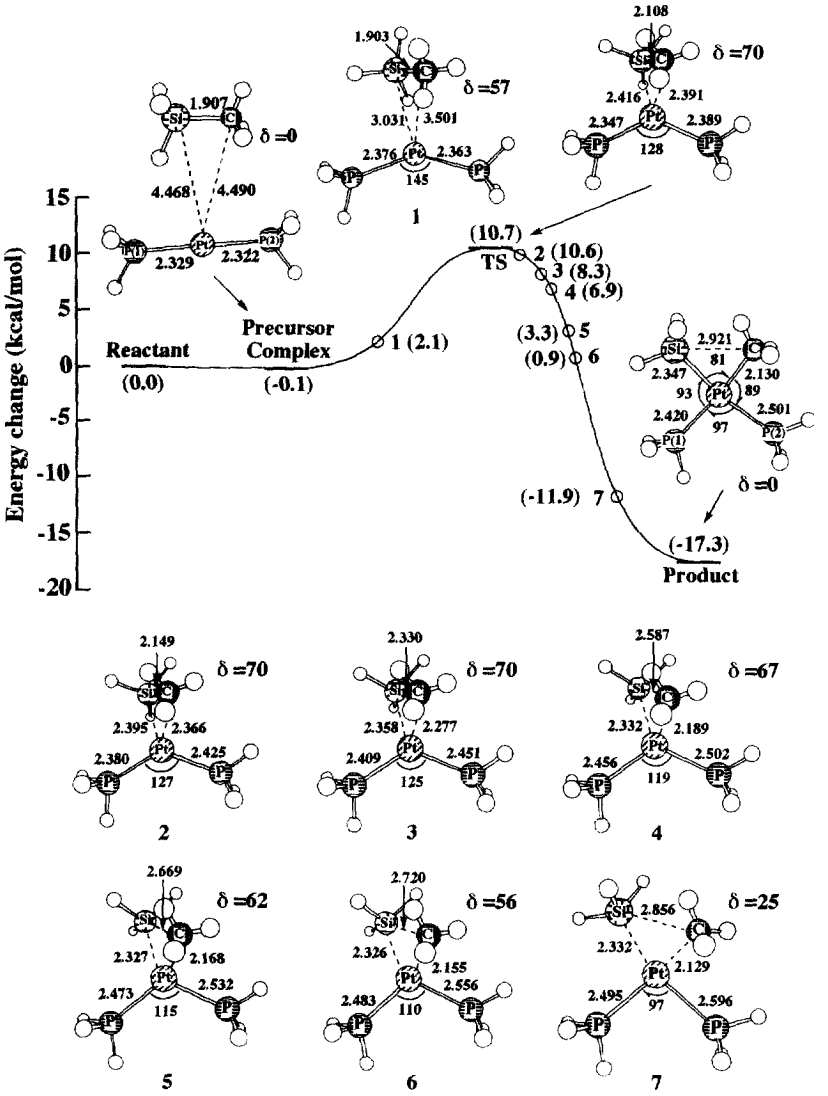

Fig. 7. Changes of total energy and geometry in the SiH_3–CH_3 reductive elimination from *cis*-$Pt(SiH_3)(CH_3)(PH_3)_2$[a] (bond length in Å and bond angle in degree). (a) IRC calculation with the MP2/BS I method.

next problem is the reason why the transition state of Si–C reductive elimination is non-planar. In Fig. 6(B), the transition state structures of $SiMe_3$–CH_3 and $SiCl_3$–CH_3 reductive eliminations are compared with that of SiH_3–CH_3 reductive elimination. The dihedral angle increases in the order SiH_3–CH_3 < $SiMe_3$–CH_3 < $SiCl_3$–CH_3, and the Pt–Si distance becomes longer in this order, while the Pt–C distance becomes shorter in the order $SiMe_3$–CH_3 ~ SiH_3–CH_3 > $SiCl_3$–CH_3. One coherent explanation is that the steric repulsion between SiR_3 and $Pt(PH_3)_2$ lengthens the Pt–Si distance, which leads to the shortening of the Pt–C distance, and at the same time, an increase in the dihedral angle; in other words the non-planar TS is favored by the steric factor.

The C–H and Si–C reductive eliminations were also investigated with *cis*-$PtH(CH_3)(PH_3)(C_2H_4)$ and *cis*-$Pt(CH_3)(SiH_3)(PH_3)(C_2H_4)$, respectively. Again, the TS of the C–H reductive elimination is planar (Fig. 6(A)), while the TS of the Si–C reductive elimination is non-planar (Fig. 6(C)). The C=C double bond is almost coplanar with the Pt–P bond in both TSs of C–H and Si–C reductive eliminations.

The Si–C reductive elimination of $Pt(SiH_3)(CH_3)(PH_3)(C_2H_4)$ occurs with a lower E_a (11.1 kcal mol^{-1}) than that (24.3 kcal mol^{-1}) of $Pt(SiH_3)(CH_3)(PH_3)_2$. The C–H reductive elimination of $PtH(CH_3)(PH_3)(C_2H_4)$ also occurs with a lower E_a value (9.9 kcal mol^{-1}) than that (17.7 kcal mol^{-1}) of $PtH(CH_3)(PH_3)_2$. These results are consistent with the experimental results of Ozawa et al. [48] that the Si–C reductive elimination of $Pt(CH_3)(SiPh_3)(PMePh_2)_2$ is accelerated by substituting electron-withdrawing alkyne for $PMePh_2$. The reason is easily interpreted in terms of the back-donating interaction shown in Fig. 6(C). Although one Pt d orbital is destabilized by an anti-bonding overlap with a PH_3 lone pair orbital, the C=C σ^* orbital forms a π-back donating interaction with the Pt d orbital, which stabilizes the transition state and facilitates the reductive eliminations from $PtH(CH_3)(PH_3)(C_2H_4)$ and $Pt(SiH_3)(CH_3)(PH_3)(C_2H_4)$. In $PtH(CH_3)(PH_3)_2$ and $Pt(SiH_3)(CH_3)(PH_3)_2$, such a π-back donating interaction cannot be formed, since PH_3 does not have a good acceptor orbital. Thus, reductive eliminations from $PtH(CH_3)(PH_3)(C_2H_4)$ and $Pt(SiH_3)(CH_3)(Ph_3)(C_2H_4)$ can occur with a lower activation energy than those of $PtH(CH_3)(PH_3)_2$ and $Pt(SiH_3)(CH_3)(PH_3)_2$.

8. Energy changes along Chalk–Harrod and modified Chalk–Harrod mechanisms

We have made all the preparations for investigating energy changes along catalytic cycles of the Chalk–Harrod and modified Chalk–Harrod mechanisms. Energy changes are shown in Figs. 8 and 9, in which the energy change by associative PH_3–C_2H_4 substitution of $PtH(SiR_3)(PH_3)_2$ is given since the dissociative substitution requires a much higher destabilization energy than the associative substitution.

As shown in Fig. 8(A), the rate-determining step of the Chalk–Harrod mechanism is the isomerization of the ethylene insertion product, whose barrier is about 22 kcal mol^{-1} for R = H and Me, and 26 kcal mol^{-1} for R = Cl. On the other hand, the rate-determining step of the modified Chalk–Harrod mechanism without

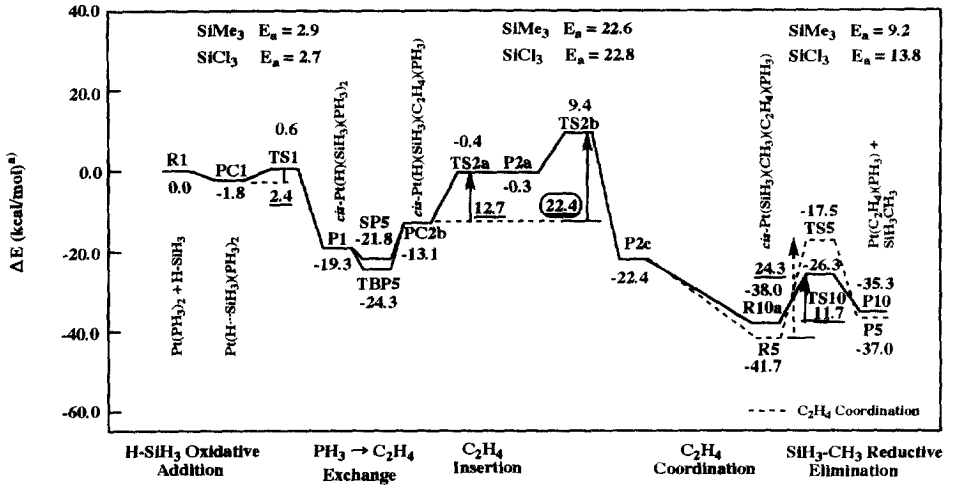

(A) Chalk-Harrod mechanism

------ **PH_3 Coordination**[b)]

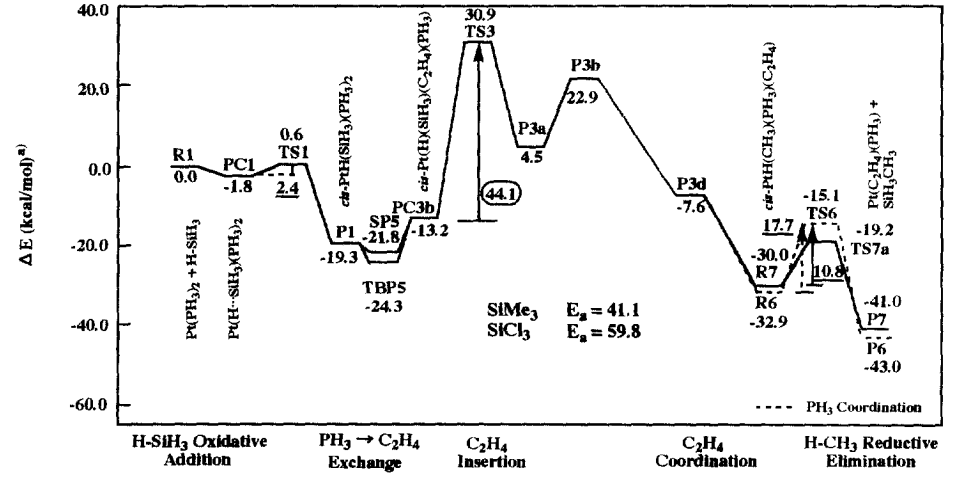

(B) Modified Chalk-Harrod mechanism

------ **PH_3 Coordination**[a)]

Fig. 8. Energy changes[(a)] along the Chalk–Harrod and modified Chalk–Harrod mechanisms without the *cis–trans* isomerization of $PtH(SiH_3)(PH_3)_2$. (a) kcal mol^{-1} with MP4SDQ. (b) Dotted lines represent the Si–C reductive elimination from $Pt(SiH_3)(CH_3)(PH_3)_2$ and the C–H reductive elimination from $PtH(CH_3)(PH_3)_2$, while solid lines mean the Si–C reductive elimination from $Pt(SiH_3)(CH_3)(PH_3)(C_2H_4)$ and the C–H reductive elimination from $PtH(CH_3)(PH_3)(C_2H_4)$.

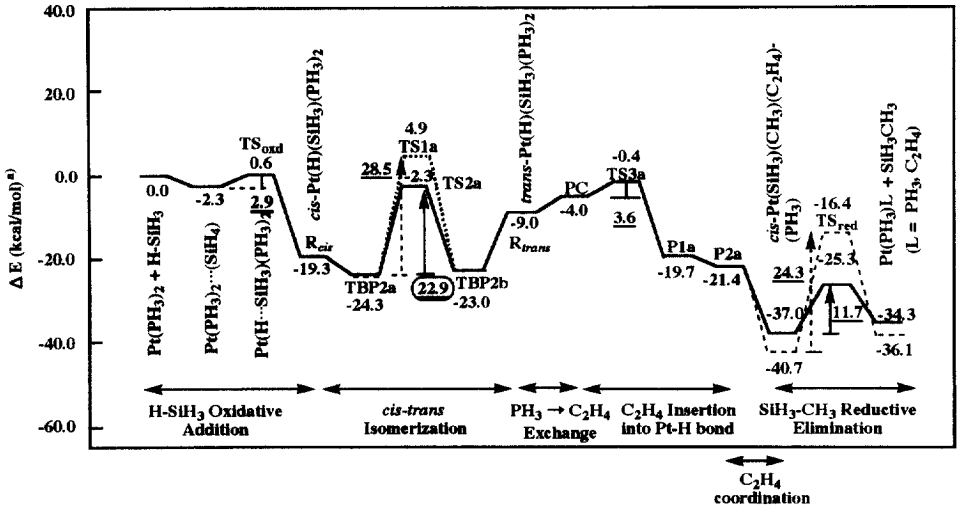

(A) Chalk-Harrod mechanism including the *cis-trans* isomerization

--- PH_3 Coordination[b)]

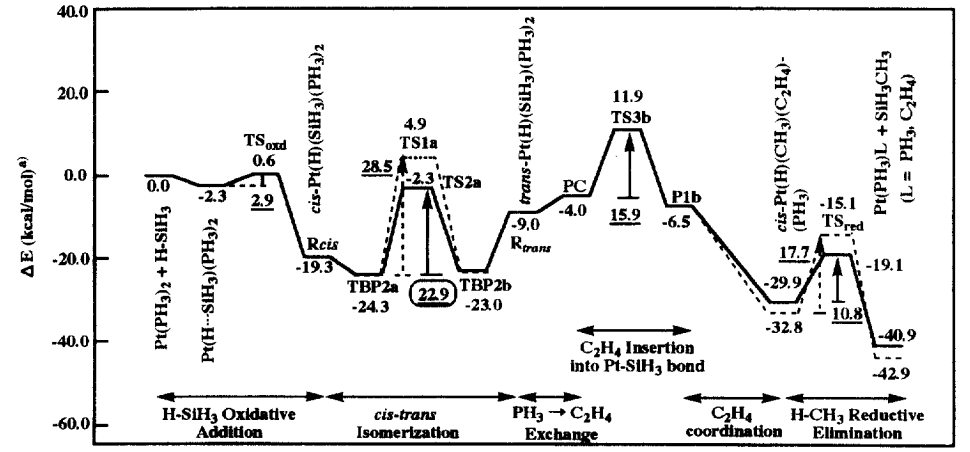

(B) Modified Chalk-Harrod mechanism including the *cis-trans* isomerization

--- PH_3 Coordination[b)]

Fig. 9. Energy changes[a)] along the Chalk–Harrod and modified Chalk–Harrod mechanisms including the *cis–trans* isomerization of $PtH(SiH_3)(PH_3)_2$. (a) kcal mol^{-1} with MP4SDQ. (b) Dotted lines represent the PH_3-promoted *cis–trans* isomerization, the Si–C reductive elimination from $Pt(SiH_3)(CH_3)(PH_3)_2$, and the C–H reductive elimination from $PtH(CH_3)(PH_3)_2$, while the solid lines mean the C_2H_4-promoted *cis–trans* isomerization, the Si–C reductive elimination from $Pt(SiH_3)(CH_3)(PH_3)(C_2H_4)$, and the C–H reductive elimination from $PtH(CH_3)(PH_3)(C_2H_4)$.

the *cis–trans* isomerization is the ethylene insertion into Pt–SiR_3, whose barrier is about 44 kcal mol^{-1} for R = H, 41 kcal mol^{-1} for R = Me, and 60 kcal mol^{-1} for R = Cl. Thus, it is clearly concluded that the Chalk–Harrod mechanism is more favorable than the modified Chalk–Harrod mechanism.

Energy changes in the reaction mechanism including the *cis–trans* isomerization are shown in Fig. 9(A) and (B), where only the R = H system was investigated. In the *cis–trans* isomerization we investigated two possibilities; in one, PH_3 promotes the *cis–trans* isomerization, and in the other, C_2H_4 promotes the isomerization. If PH_3 exists enough in excess to promote the *cis–trans* isomerization, PH_3 would coordinate to $Pt(CH_3)(SiH_3)(PH_3)$ and $PtH(CH_3)(PH_3)$, and therefore, the final Si–C and C–H reductive eliminations occur from *cis*-$Pt(CH_3)(SiH_3)(PH_3)_2$ and *cis*-$PtH(CH_3)(PH_3)_2$, respectively. The energy change of this case is shown by dotted lines in Fig. 9(A) and (B). The rate-determining step is the *cis–trans* isomerization in both the Chalk–Harrod and modified Chalk–Harrod mechanisms, whose activation barrier is 28 kcal mol^{-1}. This barrier is higher than the rate-determining step of the usual Chalk–Harrod mechanism without the *cis–trans* isomerization. If C_2H_4 exists enough in excess to promote the *cis–trans* isomerization, C_2H_4 would coordinate to $Pt(CH_3)(SiH_3)(PH_3)$ and $PtH(CH_3)(PH_3)$, and therefore, the Si–C and C–H reductive eliminations occur from *cis*$Pt(CH_3)(SiH_3)(PH_3)(C_2H_4)$ and *cis*-$PtH(CH_3)(PH_3)(C_2H_4)$, respectively. Energy changes are given by solid lines in Fig. 9(A) and (B). Again, the rate-determining step is the *cis–trans* isomerization in both the Chalk–Harrod and modified Chalk–Harrod mechanisms. Its barrier was estimated to be 22 kcal mol^{-1}, which is in a similar degree to the E_a value of the rate-determining step of the usual Chalk–Harrod mechanism without the *cis–trans* isomerization. Since the modified Chalk–Harrod mechanism without the *cis–trans* isomerization needs an activation energy of 41–60 kcal mol^{-1} for the ethylene insertion into Pt–SiR_3, the modified Chalk–Harrod mechanism with the *cis–trans* isomerization is much more favorable than the modified Chalk–Harrod mechanism without the *cis–trans* isomerization. However, the Chalk–Harrod mechanism is more favorable than the modified Chalk–Harrod mechanism, even if the *cis–trans* isomerization is involved in the catalytic cycle. This is because ethylene is more easily inserted into Pt–H than that into Pt–SiH_3, even in *trans*-$PtH(SiH_3)(PH_3)(C_2H_4)$. Thus, the $Pt(PH_3)_2$-catalyzed hydrosilylation of ethylene takes place mainly through the Chalk–Harrod mechanism, while some part of the reaction proceeds through the modified Chalk–Harrod mechanism including the *cis–trans* isomerization.

9. Conclusions

Platinum(0)-catalyzed hydrosilylation of ethylene was theoretically investigated with ab initio MO/MP2-MP4SDQ and CCD methods, in which two representative reaction mechanisms, Chalk–Harrod and modified Chalk–Harrod mechanisms, were mainly discussed. In both mechanisms, the first step is the Si–H oxidative addition of $HSiR_3$ (R = H, Me, or Cl) to $Pt(PH_3)_2$ which occurs with a very small

activation barrier (2–3 kcal mol^{-1}). In the Chalk–Harrod mechanism, the ethylene insertion into Pt–H of *cis*-$PtH(SiR_3)(PH_3)$ and the Si–C reductive elimination from *cis*-$Pt(CH_3)(SiR_3)(PH_3)(C_2H_4)$ occur with moderate barriers (10–14 and 7–12 kcal mol^{-1}, respectively). The rate-determining step is the isomerization of the ethylene insertion product which exhibits a barrier of 22–26 kcal mol^{-1}. In the modified Chalk–Harrod mechanism, the rate-determining step is the ethylene insertion into $Pt–SiR_3$ which exhibits a barrier of 44–60 kcal mol^{-1}, whereas the C–H reductive elimination from *cis*-$PtH(CH_3)(PH_3)(C_2H_4)$ occurs with a moderate barrier (9.9 kcal mol^{-1}). Since the rate determining step of the Chalk–Harrod mechanism has a lower barrier than that of the modified Chalk–Harrod mechanism, it is reasonably concluded that $Pt(PH_3)_2$-catalyzed hydrosilylation of ethylene takes place through the Chalk–Harrod mechanism.

The reaction mechanism including *cis–trans* isomerization of $PtH(SiH_3)(PH_3)_2$ was also theoretically investigated. The C_2H_4-promoted isomerization occurs via Berry's pseudo-rotation mechanism with a barrier of about 22 kcal mol^{-1}. The barrier of the PH_3-promoted isomerization is higher than that of C_2H_4-promoted isomerization, because PH_3 does not have a good acceptor orbital. The ethylene insertion into Pt–H and $Pt–SiH_3$ (E_a = 3.6 and 15.9 kcal mol^{-1}, respectively), the Si–C reductive elimination from *cis*-$Pt(SiH_3)(CH_3)(PH_3)(C_2H_4)$, and the C–H reductive elimination from *cis*-$PtH(CH_3)(PH_3)(C_2H_4)$ occur with a lower barrier (11.1 and 9.9 kcal/mol, respectively) than that of the *cis–trans* isomerization. Thus, the *cis–trans* isomerization is the rate-determining step in the Chalk–Harrod and modified Chalk–Harrod mechanisms if the *cis–trans* isomerization is involved in the mechanism. Since the barrier of the C_2H_4-promoted *cis–trans* isomerization is almost the same as the barrier for the isomerization of the ethylene insertion product which is the rate-determining step in the Chalk–Harrod mechanism without the *cis–trans* isomerization, the $Pt(PH_3)_2$-catalyzed hydrosilylation of ethylene might proceed through the modified Chalk–Harrod mechanism when the *cis–trans* isomerization of $PtH(SiH_3)(PH_3)_2$ occurs. Of course the Chalk–Harrod mechanism is more favorable than the modified Chalk–Harrod mechanism even if the *cis–trans* isomerization is involved, since ethylene is more easily inserted into Pt–H than that into $Pt–SiH_3$ even in *trans*-$PtH(SiH_3)(PH_3)(C_2H_4)$.

We also mention here several important results presented for each elementary step of Pt-catalyzed hydrosilylation of olefin. (1) The transition states of Si–H oxidative addition to $Pt(PH_3)_2$ and C–H reductive elimination from $PtH(CH_3)(PH_3)_2$ are planar, while the transition state of Si–C reductive elimination is non-planar against expectation from the orbital interaction diagram. This is understood in terms of steric repulsion between SiR_3 and $Pt(PH_3)_2$. (2) The Si–C reductive elimination from Pt(II) complex is accelerated by coordination of ethylene instead of PH_3. This is because the π-back donating interaction between Pt d and C_2H_4 π* orbitals stabilizes the transition state. (3) The C_2H_4 promoted *cis–trans* isomerization of $PtH(SiH_3)(PH_3)_2$ occurs through a Berry's pseudo-rotation mechanism with a lower E_a value than does the PH_3-promoted isomerization. The reason is that C_2H_4 stabilizes the trigonal bipyramidal transition state by a π-back donating interaction.

Acknowledgements

This work was financially supported in part by the Ministry of Education, Culture, Sports, and Science through Grants-in-Aid for Scientific Research on Priority Area.

References

[1] (a) J.L. Speier, Adv. Organomet. Chem. 17 (1979) 407. (b) J.F. Harrod, A.J. Chatt, in: I. Wender, P. Pino (Eds.), Organic Synthesis via Metal Carbonyls, Wiley, New York, 1977. (c) T.D. Tilley, in: S. Patai, Z. Rappoport (Eds.), The Chemistry of Organic Silicon Compounds, Wiley, New York, 1989, p. 1415. (d) I. Ojima, in: S. Patai, Z. Rappoport (Eds.), The Chemistry of Organic Silicon Compounds, Wiley, New York, 1989, p. 1479.
[2] (a) J.L. Speier, J.A. Webster, G.H. Barnes, J. Am. Chem. Soc. 79 (1957) 974. (b) J.C. Saam, J.L. Speier, J. Am. Chem. Soc. 80 (1958) 1404. (c) J.W. Ryan, J.L. Speier, J. Am. Chem. Soc. 86 (1964) 895.
[3] A.J. Chalk, J.F. Harrod, J. Am. Chem. Soc. 87 (1965) 16.
[4] (a) M.A. Schrooder, M.S. Wrighton, J. Organomet. Chem. 128 (1977) 345. (b) C.L. Reichel, M.S. Wrighton, Inorg. Chem. 19 (1980) 3858. (c) C.L. Randolph, M.S. Wrighton, J. Am. Chem. Soc. 108 (1986) 3366.
[5] (a) A. Milan, E. Towns, P.M. Maitlis, J. Chem. Soc. Chem. Commun. (1981) 673. (b) A. Milan, M.-J. Fernandez, P. Bentz, P.M. Maitlis, J. Mol. Catal. 24 (1984) 89.
[6] I. Ojima, M. Yatabe, T. Fuchikami, J. Organomet. Chem. 260 (1984) 335.
[7] S.B. Duckett, R.N. Perutz, Organometallics 11 (1992) 90.
[8] M.A. Esteruelas, J. Herrero, L.A. Oro, Organometallics 12 (1993) 2377.
[9] (a) M.J. Hostetler, R. Bergman, J. Am. Chem. Soc. 112 (1990) 8621. (b) M.J. Hostetler, M.D. Butts, R. Bergman, Organometallics 12 (1993) 65.
[10] M.A. Esteruelas, M. Olivan, L.A. Oro, Organometallics 12 (1993) 65.
[11] T. Takahashi, M. Hasegawa, N. Suzuki, M. Saburi, C.J. Rousset, P.E. Fanwick, E. Negishi, J. Am. Chem. Soc. 113 (1991) 8564.
[12] P.F. Fu, L. Brard, Y. Li, T.J. Marks, J. Am. Chem. Soc. 117 (1995) 7157.
[13] (a) K. Yamamoto, T. Hayashi, M. Kumada, J. Organomet. Chem. 28 (1971) C37. (b) K. Yamamoto, T. Hayashi, M. Kumada, J. Am. Chem. Soc. 93 (1971) 5301.
[14] (a) M. Green, J.L. Spencer, C.A. Tsipis, J. Chem. Soc. Dalton Trans. 1519 (1977) 1525. (b) C.A. Tsipis, J. Organomet. Chem. 187 (1980) 427. (c) C.A. Tsipis, J. Organomet. Chem. 188 (1980) 53.
[15] A.L. Pignato, W.C. Trogler, J. Am. Chem. Soc. 109 (1987) 3586.
[16] Y. Uozumi, K. Kitayama, T. Hayashi, K. Yanagi, E. Fukuyo, Bull. Chem. Soc. Jpn. 38 (1995) 713.
[17] S. Sakaki, N. Mizoe, M. Sugimoto, Organometallics 17 (1998) 2510.
[18] B.M. Bode, P.N. Day, M.S. Gordon, J. Am. Chem. Soc. 120 (1998) 1552.
[19] (a) H.C. Clark, H. Kurosawa, Inorg. Chem. 11 (1972) 1275. (b) H.C. Clark, C. Jablonski, J. Halpern, A. Mantovani, T.A. Well, Inorg. Chem. 13 (1974) 1541. (c) H.C. Clark, C.R. Jablonski, Inorg. Chem. 13 (1974) 2213. (d) H.C. Clark, C.S. Wong, J. Am. Chem. Soc. 96 (1974) 7213. (e) H.C. Clark, C.R. Jablonski, C.S. Wong, Inorg. Chem. 14 (1975) 1332.
[20] Y. Ben-David, M. Portnoy, M. Gozin, D. Milstein, Organometallics 11 (1992) 1995.
[21] S.P. Ermer, G.E. Struck, S.P. Bitler, R. Richards, R.R. Bau, T.C. Flood, Organometallics 13 (1993) 2634.
[22] D.L. Reger, D.G. Garza, L. Lebioda, Organometallics 11 (1992) 4285.
[23] D.L. Thorn, R. Hoffmann, J. Am. Chem. Soc. 100 (1978) 2079.
[24] N. Koga, S.Q. Jin, K. Morokuma, J. Am. Chem. Soc. 110 (1988) 3417.
[25] S. Sakaki, M. Ogawa, Y. Musashi, T. Arai, J. Am. Chem. Soc. 116 (1994) 7258.

[26] (a) R.S. Berry, J. Chem. Phys. 32 (1960) 933. (b) E.L. Mutterties, J. Am. Chem. Soc. 91 (1969) 1636, 4115.
[27] J. Chatt, B.L. Shaw, J. Chem. Soc. (1959) 4020.
[28] S. Sakaki, M. Ogawa, M. Kinoshita, J. Phys. Chem. 99 (1995) 9933.
[29] P.J. Hay, W.R. Wadt, J. Chem. Phys. 82 (1985) 299.
[30] W.R. Wadt, P.J. Hay, J. Chem. Phys. 82 (1985) 284.
[31] S. Huzinaga, J. Andzelm, M. Klobkowski, E. Radzio-Andzelm, Y. Sakai, H. Tatewaki, Gaussian Basis Sets for Molecular Calculations, Elsevier, Amsterdam, 1984.
[32] T.H. Dunning, P.J. Hay, in: H.F. Schaefer (Ed.), Methods of Electronic Structure Theory, Plenum, New York, 1977, p. 1.
[33] K. Raghavachari, J. Chem. Phys. 32 (1985) 933.
[34] K. Fukui, Acc. Chem. Res. 14 (1981) 363.
[35] A.M.J. Frisch, G.W. Trucks, H.B. Schlegel, P.M.W. Gill, B.G. Johnson, M.A. Robb, J.R. Cheeseman, T.A. Keith, G.A. Petersson, J.A. Montgomery, K. Raghavachari, M.A. Al-Laham, V.G. Zakrzewski, J.V. Ortiz, J.B. Foreesman, J. Cioslowski, B.B. Stefanov, A. Nanayakkara, M. Challacombe, C.Y. Peng, P.Y. Ayala, W. Chen, M.W. Wong, J.L. Angres, E.S. Replogle, R. Gomperts, R.L. Martin, D.J. Fox, J.S. Binklev, D.J. DeFrees, J. Baker, J.J.P. Stewart, M. Head-Gordon, C. Gonzalez, J.A. Pople, Gaussian 94, Gaussian Inc., Pittsburgh, PA, 1995.
[36] S. Sakaki, N. Mizoe, Y. Musashi, B. Biswas, M. Sugimoto, J. Phys. Chem. A 41 (1998) 8027.
[37] K. Tatsumi, R. Hoffmann, A. Yamamoto, J.K. Stille, Bull. Chem. Soc. Jpn. 54 (1981) 1857.
[38] T.A. Albright, R. Hoffmann, J.C. Thibeault, D.L. Thorn, J. Am. Chem. Soc. 101 (1979) 3801.
[39] J. Chatt, C. Eaborn, S.D. Ibekwe, P.N. Kapoor, J. Chem. Soc. (A) (1970) 1343.
[40] S. Sakaki, N. Mizoe, Y. Musashi, and M. Sugimoto, J. Mol. Struct. (Theochem.), to be published.
[41] A.R. Rossi, R. Hoffmann, Inorg. Chem. 14 (1975) 365.
[42] Z. Lin, M.B. Hall, Inorg. Chem. 30 (1991) 646.
[43] (a) N. Koga, S. Obara, K. Morokuma, 106 (1984) 4625. (b) S. Obara, N. Koga, K. Morokuma, J. Organomet. Chem. 270 (1984) C33. (c) N. Koga, S. Obara, K. Kitaura, K. Morokuma, J. Am. Chem. Soc. 107 (1985) 7109.
[44] (a) S. Sakaki, K. Ohkubo, Organometallics 8 (1989) 2970. (b) S. Sakaki, Y. Musashi, Inorg. Chem. 34 (1995) 1914.
[45] M.R.A. Blomberg, U. Brandemark, P.E. Sieghahn, J. Am. Chem. Soc. 105 (1983) 5557.
[46] J.Y. Saillard, R. Hoffmann, J. Am. Chem. Soc. 106 (1984) 2006.
[47] (a) J.J. Low, W.A. Goddard, Organometallics 5 (1986) 609. (b) J.J. Low, W.A. Goddard, J. Am. Chem. Soc. 108 (1986) 6115.
[48] F. Ozawa, T. Hikida, T. Hayashi, J. Am. Chem. Soc. 116 (1994) 2844.